INTERNATIONAL JOURNAL OF AUTOMOTIVE AND MECHANICAL ENGINEERING
ISSN: 2229-8649 e-ISSN: 2180-1606
VOL. 21, ISSUE 2, 2024, 11235 – 11246
DOI: https://doi.org/10.15282/ijame.21.2.2024.5.0868

RESEARCH ARTICLE

Implementation of a Semi-active Auxiliary Axle for Lateral Stability of Articulated Heavy Vehicles at Extreme Loss of Control Limit

Mohammad Ismaeel Assadi*, Behrooz Mashahdi, Saleh Kasiri Bidhandi

School of Automotive Engineering, Iran University of Science and Technology, Tehran, Iran

ABSTRACT - Articulated heavy vehicles (AHVs) play a vital role in the economy of freight transport. Lateral stability control of AHVs during the immediate vicinity to loss of control (LOC) is a significant issue that has not been effectively addressed in the literature. This paper presents a novel approach to the lateral stability control of tractor semi-trailers under conditions leading to LOC. An active auxiliary axle is proposed to prevent trailer swing and snaking during severe lane change maneuvers. A linear 3-DOF model was developed to represent the effectiveness of the active auxiliary axle and tire cornering stiffness in yaw-rate control to provide an analytical basis. Nonlinear modeling of the axle and vehicle system was performed in TruckSIM. A Fuzzy Logic Controller (FLC) was developed to identify the required rate (magnitude per unit time) of actuation force, and a PID controller was introduced to regulate the magnitude of actuation force at the axle-wheel interface. Co-simulation was performed in MATLAB/SIMULINK in combination with TruckSIM. To simulate an LOC on a dry road with a coefficient of friction of 0.85, a double lane change (DLC) maneuver at 90 km/h was conducted. This resulted in a combined state of relative roll-over and trailer swing, facilitating the evaluation of the semi-active auxiliary axle's performance in regaining stability and eliminating transient overshoots in the vehicle combination's lateral response. Yaw rate rearward amplification was effectively controlled, and articulation angle oscillations were significantly diminished. This approach suggests a systematically minimal yet practicable retrofit to the trailer, contributing to a remarkable improvement in the traffic safety of AHVs.

ARTICLE HISTORY

Received	:	27th July 2023
Revised	:	11th Oct. 2023
Accepted	:	08th Feb. 2024
Published	:	20th June 2024

KEYWORDS

Yaw stability
Articulated heavy vehicles
Fuzzy logic controller
Active auxiliary axle

1.0 INTRODUCTION

Articulated heavy vehicles (AHVs) comprise a significant share of freight transport [1]. The articulation joint in this category of vehicles causes lateral instabilities in the form of jack-knifing, trailer swing, and snaking [2]. Various studies have addressed the lateral stability of AHVs and heavy trucks. Fancher [3] emphasized that poor choices of vehicle parameters (geometry, suspension parameters, and tire parameters) promote static (monotonic) instability. The most crucial geometrical property affecting vehicle yaw stability is the distance between the trailer's center of gravity and the rear axle midpoint. For a given set of tires, the larger the vehicle wheelbase and the higher the vehicle's forward speed, the more prone the vehicle is to exhibit static instability in the yaw plane [4]. To ensure the vehicle's stability during downhill turning maneuvers, the maximum allowable CoG distance from the rear axle midpoint should fundamentally decrease. This is reflected in [5].

The principal mechanism responsible for the onset of yaw divergence in heavy trucks and vehicles is one or a combination of the following: a) cornering stiffness behavior of tires concerning vertical load distribution and their nonlinearity, b) fore-aft suspension roll stiffness distribution, and c) high center of gravity and elevated speeds [6]. Winkler [7] proposed four ways to address lateral instability: modification of fore-aft suspension stiffness, lowering the center of gravity of the vehicle-load combination, incorporation of additional tires at the rear, and introduction of tires with more linear-like cornering force generation behavior. Various methods have been developed to enhance the lateral performance of AHVs. Cebon et al. [8] categorized AHVs' dynamic stability systems into four groups: (1) active suspension systems, (2) active trailer steering, (3) differential braking, and (4) active front steering.

Truck tires represent a relatively low slope in the lateral force vs. slip angle curve, and a large angle is required for them to reach maximum cornering force [9]. In lightly loaded conditions, the principal mechanism governing high-speed instability is the nonlinear behavior of tire cornering force concerning vertical load. Additionally, the maximum cornering force at rear truck tires is lower than at front tires and exhibits more nonlinearity [10]. The cornering stiffness of the nearest axles to the articulation point has the highest contribution to vehicle lateral performance [11], and increasing it via material properties modification [12] significantly improves yaw rate rearward amplification (RWA). Wu and Lin [13] showed that during high-speed transient maneuvers, the time response of the system to generate the required lateral force is a determinant factor for stability. The delay occurring in the development of non-steered rear axles concerning the front steering axles causes RWA as well as a delayed perception of the situation by the driver [14].

Decreased cornering stiffness at trailer axles provokes trailer swing or snaking. The best performance in the lateral load generation of tires is achieved when the total capacity of the tire is employed. Divergent lateral instability results

***CORRESPONDING AUTHOR | Mohammad Ismaeel Assadi** | ✉ m_assadi@alumni.iust.ac.ir

from the reduced lateral force generation of trailer tires. Therefore, at the verge of instability, there are only two possibilities for regaining stability: increased lateral force by means of increased vertical load or imposing a counteracting yaw moment to prevent divergent oscillations.

Steering of the trailer wheels has been proposed and implemented in many studies with promising responses for both low-speed maneuverability and high-speed stability [13-15] and [19-21]. Applications of active trailer steering for improved high-speed cornering and roll stability of articulated heavy vehicles were proposed by Cebon et al. [17] and Cheng and Cebon [18], respectively. Nonetheless, the system is functionally complex and imposes significant costs. Additionally, the steering system alone is incapable of utilizing the potential of tires to their full capacity [16]. Differential braking systems proposed under various terminologies [22-25] have superior functionality with the highest power density, high fidelity, existing technology, and minimal retrofit required. The application of differential braking to prevent jack-knifing and roll-over was addressed in [26-28]. The only limitation of braking systems such as yaw stability control is that path-tracking maneuverability is sacrificed. Roll stability of articulated heavy vehicles through active suspension and active anti-roll bars has been discussed in [29] and [30] with implications for coupled yaw dynamics.

The application of computer simulation tools, including truckSIM and MSC ADAMS, has facilitated both nonlinear modeling and model verification in the analytical study of AHVs. Ahmadi Jeyed and Ghaffari [31] validated a nonlinear 4-DOF model of AHVs against a 21-DOF model in truckSIM and used it to develop an estate estimation program using an extended Kalman filter (EKF). Junior et al. used a linear AHVs model to regulate path-following off-tracking (PFOT) in combination with a robust LQR regulator. The performance of the proposed model was studied against a comparable H_∞ model [32]. Xu et al. developed a switchable control algorithm to ascertain low-speed PFOT and high-speed lateral stability using LQR with different control tunes [33]. Active yaw stability control of a car-trailer combination using an experimental full-scale model was studied by Sorniotti et al. The authors used gain scheduling for optimal yaw rate reference generation based on the state measurement of hitch angle via a hitch angle sensor and used a PI controller on the towing vehicle to regulate the hitch angle by torque vectoring [34]. Zhang et al. [35] developed a yaw stability controller for articulated vehicles based on a two-layer controller with differential braking systems capable of being introduced to other vehicle models. They used the upper-level model predictive controller (MPC) to identify the required corrective action for the vehicle combination and a lower-level control allocation (CA) to distribute yaw corrective moment generation among desired tires of the vehicle.

The dependency of these methods on effective contact between original tires and the road, on one side, and the limitation in the combination of vertical load and friction, restricts their performance in instances including saturation of tire forces, side-wheel lift-off, or insufficient vertical force on the tires. While the proposed methods have been successful in conferring stability and significantly reducing traffic hazards with their industrial applications already on the market, the problem with high-speed lateral stability after LOC incidents has not been effectively addressed in AHVs. Indeed, the proposed systems work well as long as the vehicle is within a limited boundary of instability.

Our study aims to rely on the premise of the classical findings, i.e., the effect of tire cornering stiffness and the distance of the active auxiliary axle from the hitch point, to investigate the following: a) To what extent will the combination of tire properties modification and axle location be effective in regaining stability and preventing loss of control (LOC) in severe obstacle-avoidance maneuvers where lateral instability occurs? b) Does existing technology, including semi-active suspension design and modified tire properties, have the potential to be introduced as a retrofit to the existing system to assist the vehicle combination in recovering stability after an LOC incident?

In this regard, we have introduced a new approach that constitutes a retrofit of active actuators to an axle, replacing the conventional tag axle with tires with modified cornering stiffness toward more linear-like lateral force generation behavior to help the vehicle stabilize in critical handling situations. Our paper is structured as follows: Section one reviews existing literature and contributes to our study. Section two introduces an active auxiliary axle concept with modified tire properties. Section three presents our proposed active axle model. Section four details control system development. Section five discusses the results, and section six provides concluding remarks.

2.0 FUNCTION OF A SEMI-ACTIVE AUXILIARY AXLE

The proposed method consists of an auxiliary axle equipped with tires of modified cornering stiffness curve towards more linearity (high stiffness tires), which is closer to the hitch point. By having active actuators, it employs controlled vertical force (and the most desired utilization of tire force generation potential). Figure 1(a) represents the function of the proposed active auxiliary axle in generating a stabilizing yaw moment around the hitch point and in the opposite direction to the yaw divergent moment. The axle location was determined in a previous study by the authors using a nonlinear model developed in truckSIM [37]. As the trailer tires saturate in the lateral direction, causing it to experience lateral oscillations, the semi-active axle is actuated to generate the lost lateral grip and exert a yaw-stabilizing moment on the trailer. The axle tires on the left and right sides are controlled to engage independently depending on the directional attitude of the trailer. We shall emphasize that the system proposed in this study does not primarily aim to improve maneuverability or handling performance but aims to prevent high-amplitude lateral oscillations of the trailer when loss of control is perceived and original systems have lost their functionality beyond LOC. Table 1 offers vehicle parameters.

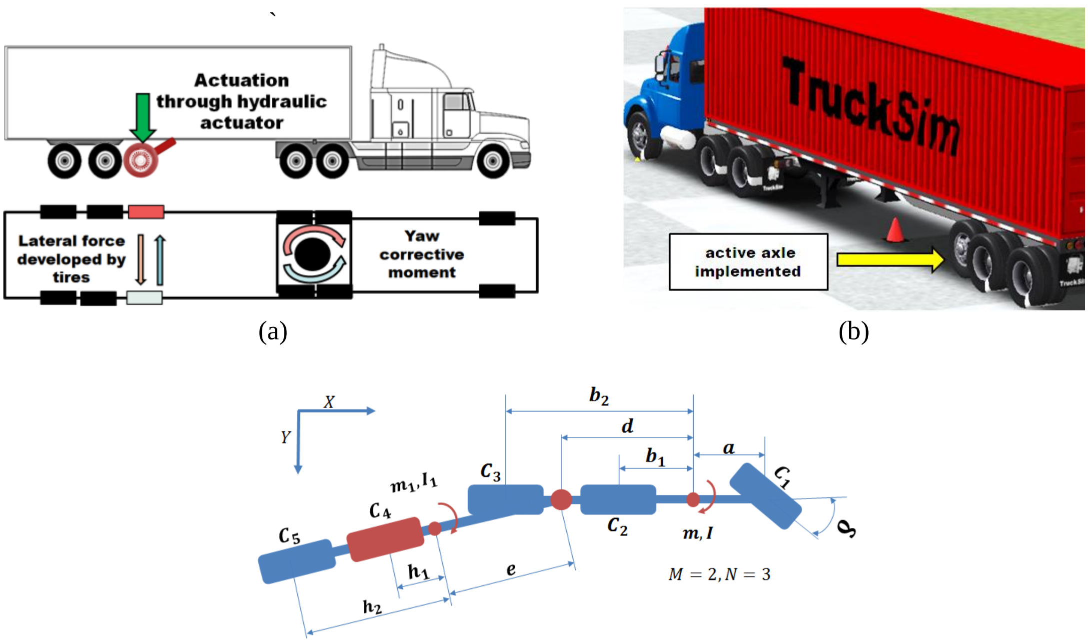

(a) (b)

(c)

Figure 1. (a) The concept of proposed active auxiliary and development of corrective yaw moment (b) The five-axle nonlinear model in truckSIM equipped with an auxiliary axle, (c) mathematical yaw plane model to represent active auxiliary axle

Table 1. Description of terms and parameters in the paper

Parameter	Description and Units	Numerical Value
$\boldsymbol{m}$	Tractor mass (kg)	8450
$\boldsymbol{m_1}$	Trailer mass (kg)	7330
$\boldsymbol{I}$	Tractor mass moment inertia in yaw plane $(\frac{kg}{m^2})$	2939412
$\boldsymbol{I_1}$	Trailer mass moment of inertia in yaw plane $(\frac{kg}{m^2})$	204188
$\boldsymbol{C_1}$	Tractor front axle tire cornering stiffness $(\frac{N}{rad})$	381930
$\boldsymbol{C_2}$, $\boldsymbol{C_3}$	Tractor rear axle tire cornering stiffness $(\frac{N}{rad})$	734000
$\boldsymbol{C_4}$	Active auxiliary axle tire cornering stiffness $(\frac{N}{rad})$	variable
$\boldsymbol{C_5}$	Semi-trailer composite axle tire cornering stiffness $(\frac{N}{rad})$	880000
$\boldsymbol{a}$	Distance between tractor front axle and tractor CoG (m)	1.143
$\boldsymbol{b_1}$	Distance between tractor CoG and middle axle (m)	1.6
$\boldsymbol{b_2}$	Distance between tractor CoG and rearmost axle (m)	2.560
$\boldsymbol{d}$	Distance between tractor CoG and hitch point location(m)	1.925
$\boldsymbol{e}$	Distance between hitch point and semi-trailer CoG (m)	3.048

Table 1. (cont.)

Parameter	Description and Units	Numerical Value
$\boldsymbol{h_1}$	Distance between hitch point and active auxiliary axle (m)	3.161
$\boldsymbol{h_2}$	Distance between hitch point trailer composite axles (m)	4.2
$\boldsymbol{\delta}$	Tractor front axle steer angle $(degs)$	2(SLC), 4.5 (DLC)
$\boldsymbol{v_x}$	Tractor forward velocity $(\frac{m}{s})$	25
$\boldsymbol{\mu}$	Coefficient of friction	0.85
$\boldsymbol{M}$	Mass matrix	
$\boldsymbol{v_{y1}}$	Tractor lateral velocity $(\frac{m}{s})$	
$\boldsymbol{r_1}$	Tractor yaw rate $(\frac{deg}{s})$	
$\boldsymbol{\gamma}$	Articulation angle $(degs)$	
$\boldsymbol{F_y}$	Lateral force (N)	
$\boldsymbol{\alpha}$	Tire side slip angle $(degs)$	
$\boldsymbol{K_u}$	Understeer gradient	
$\boldsymbol{r_{ss}}$	Steady-state yaw rate $(\frac{degs}{s})$	
$\boldsymbol{E}$	Yaw rate error $(\frac{deg}{s})$	

2.1 Analysis of Yaw Stabilizing Effect Using a Linear Model

A linear three-DOF model was developed to represent the effectiveness of the proposed model and to evaluate the effect of tire cornering stiffness modification. In the current model, a tractor semi-trailer was considered with the tractor having three axles and the trailer having two axles. The auxiliary axle was integrated into the mathematical model using a representative tire with modified cornering stiffness properties. The trailer is shown schematically with red tire prints representing the auxiliary active axle, and the two remaining axles have been considered as a single composite axle designated as C_5. The description of terms and model parameters is provided in Table 1. The equations of motion are derived using Newton's second law of motion. Two coordinate systems, one attached to the tractor (CoG) and the other to the semi-trailer CoG, have been considered to allow for the elimination of the hitch point internal force by the law of transfer of coordinates.

$$m\left(V_{\dot{y}} + V_x r\right) = F_{y1} + F_{y2} + F_{y3} - F_h \tag{1}$$

$$I r^{\cdot} = aF_{y1} - b_1 F_{y2} - b_2 F_{y2} + dF_h \tag{2}$$

$$m_1\left(V_{\dot{y}1} + V_x r_1\right) = F_{y4} + F_{y5} + F_h \tag{3}$$

$$I_1 r^{\cdot} = -h_1 F_{y4} - 2F_{y5} + eF_h \tag{4}$$

The above set of linear differential equations was solved by eliminating the hitch point force to obtain the following state-space form.

$\dot{X} = Ax + Bu$ where $A = -M^{-1}D$ and$B = M^{-1}C\delta$

$$M = \begin{bmatrix} (m+m_1) & -m_1(d+e) & m_1 e & 0 \\ m_1 e & I + m_1 d(d+e) & -m_1 ed & 0 \\ -m_1 d & I_1 + m_1 d(d+e) & -(I_1 + m_1 e^2) & 0 \\ 0 & 0 & 0 & 1 \end{bmatrix} \tag{5}$$

$$D = -\frac{1}{v_x}\begin{bmatrix} D_{11} & D_{12} & D_{13} & D_{14} \\ D_{21} & D_{22} & D_{23} & D_{24} \\ D_{31} & D_{32} & D_{33} & D_{34} \\ D_{41} & D_{42} & D_{43} & D_{44} \end{bmatrix}$$

$$D_{11} = -\sum_{i-1}^{N} C_i - \sum_{j=1}^{M} C_{N+j} \qquad D_{12} = -(m+m_1)v_x^2 + \sum_{i=2}^{N} b_{i-1}C_i + \sum_{j=1}^{M}(d+e+h_j)C_{N+j} - aC_1$$

$$D_{13} = -\sum_{j=1}^{M}(h_j+e)C_{N+j} \qquad D_{14} = -v_x\sum_{j=1}^{M} C_{N+j}$$

$$D_{21} = \sum_{i=2}^{N} b_{i-1}C_i + d\sum_{j=1}^{M} C_{N+j} - aC_1 \qquad D_{22} = m_1 d v_x^2 - a^2C_1 - \sum_{i=2}^{N} b_{i-1}^2 C_i - d\sum_{j=1}^{M}(d+e+h_j)C_{N+j} \tag{6}$$

$$D_{23} = d\sum_{j=1}^{M}(h_j+e)C_{N+j} \qquad D_{24} = v_x d\sum_{j=1}^{M} C_{N+j}$$

$$D_{31} = \sum_{j=1}^{M}(h_j+e)C_{N+j} \qquad D_{32} = m_1 e v_x^2 - \sum_{j=1}^{M}(h_1+e)(d+e+h_j)C_{N+j}$$

$$D_{33} = \sum_{J=1}^{M}(h_j+e)^2 C_{N+j} \qquad D_{34} = v_x\sum_{j=1}^{M}(h_j+e)C_{N+j}$$

$$D_{41} = D_{42} = D_{44} = 0 \qquad D_{43} = 1$$

$$X = [v_{y1}\; r_1\; \dot{\gamma}\; \gamma]^T \tag{7}$$

$$C = [C_1\; aC_1\; 0\; 0]^T \tag{8}$$

A single lane change maneuver was simulated to evaluate the yaw performance of the vehicle system in the presence of the active auxiliary axle. To determine the boundary of the tire stiffness curve for the proposed active axle, the lateral stiffness of the representative auxiliary axle was increased stepwise in four stages by one to four times the stiffness of the original tires of the model (represented by C to 4C in Figure 2(b) respectively). Zero stiffness was assumed for axle C_4, representative of a standard trailer structure. The lane change maneuver was performed at 90 km/h with the steering angle curve shown in Figure 2(a). Figure 2(b) suggests that an additional axle with increased cornering stiffness helps reduce the yaw rate of the trailer. While increased lateral stiffness by a factor of four leads to the best yaw-rate reduction of nearly 21%, a reduction with a tire of the same stiffness as that of the original trailer tires results in an 11% reduction in the yaw rate, slightly more than half the gain with a hypothetically exaggerated tire stiffness of four times the original value. This substantiates the preliminary assumption of tire cornering force modification with an axle introduced to the system. More importantly, the overly large cornering stiffness considered here does not necessarily need to be implemented in the real tire, as the magnitude of tire lateral force is a function of vertical load, which is controlled via the proposed actuator system.

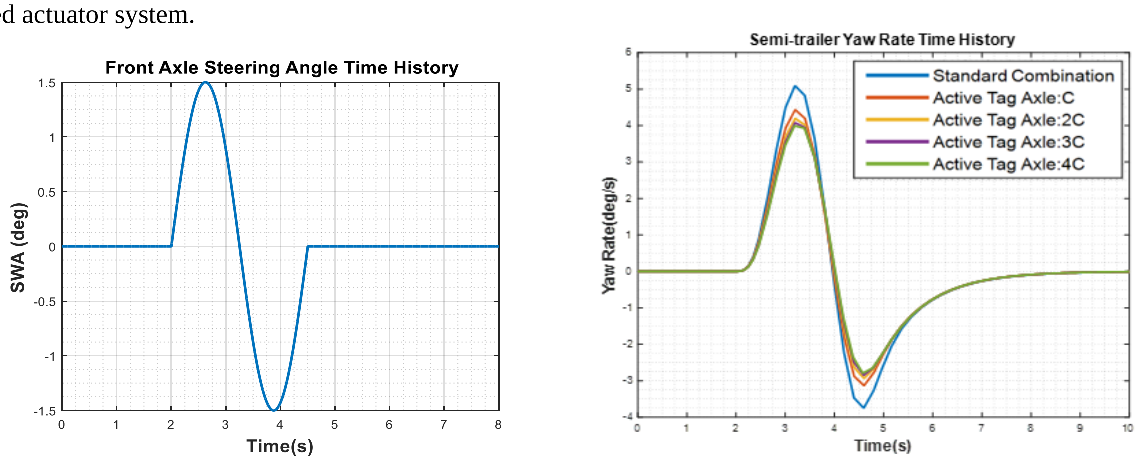

(a) (b)

Figure 2. (a) Road wheel steering angle in open-loop single lane change maneuver, (b) Semi-trailer yaw rate response at 90km/h and 1.5 degrees of road wheel steering angle for different values of cornering stiffness of active axle

Furthermore, the required tire stiffness to practically enable the system to function satisfactorily is far closer to reality than to hypothetically high values. As such, the results here conform to the reports in [36] and [11] and substantiate the approaches proposed. Additionally, the findings correspond to the results obtained in [13], where the stability of tractor semi-trailers is improved in the presence of higher cumulative cornering stiffness at trailer axles.

3.0 NONLINEAR VEHICLE SYSTEM AND TIRE MODEL

Following the results obtained in the linear model analysis, a nonlinear five-axle tractor semi-trailer combination (three axles for the tractor and two axles for the semi-trailer) was developed and implemented with an active axle modeled in truckSIM. TruckSIM allows the configuration of the vehicle to be modified using user-defined functions. TruckSIM uses an integrated nonlinear Magic Formula (MF) tire model with tabular parameters. The tire library provides user-defined functions to effectively model tire behavior for the desired function. In order to substantiate tire models, the original tire data was first compared against an experimental model offered in [36] for truck tires. The general form of the MF formula is given in Eq. (9) and was used to obtain the normalized lateral force vs. slip angle for a typical tire shown in Figure 3(b).

$$y = DSin\{C.tan^{-1}[B - E.(B - tan^{-1}(B))]\} \tag{9}$$

where B, C, D, and E are, respectively, stiffness, shape, peak, and curvature factors that serve to produce the desired curves. For the current study, the coefficients were B = 0.714, D = 1.00, C = 1.40, and E = -0.20, respectively. This results in a reasonably linear-like tire lateral force-slip angle relationship, as put forth by Winkler [7]. The results of the simulation are reported in Figure 3(b). In the next step, the tabular tire properties in the truckSIM library for the fully nonlinear model were modified to match the tire properties obtained using the MF tire model. The tire model was modified so that the saturation of lateral force would occur at smaller slip angles around 2-2.5 degrees. This ensured conformity with the performance of the linear model in section 2.1. Results for a given vertical load of 20,000N are illustrated in Figure 3(a) before and after modification of the slip angle vs lateral force behavior of the tire.

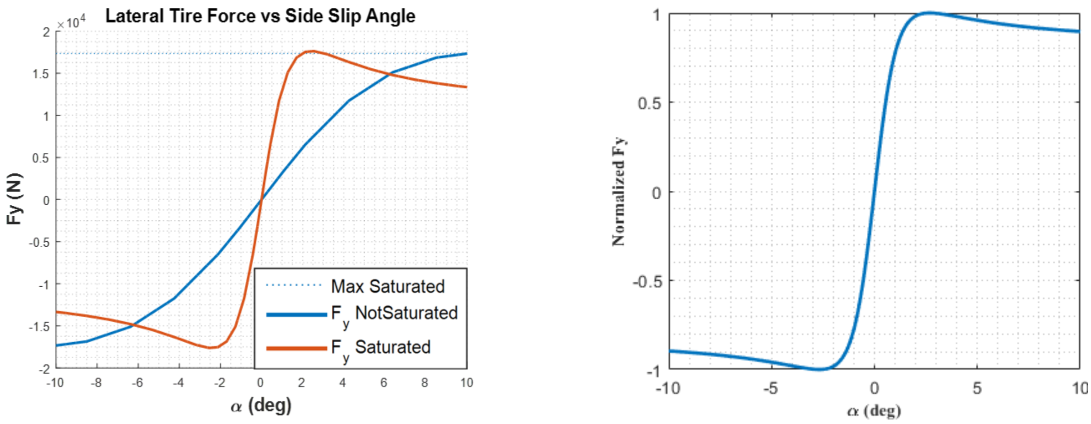

Figure 3. Tire modeling for improved lateral performance. a) Tire model in truckSIM for modified and original models. b) corresponding normalized lateral force against slip angle for MF model

As demonstrated in Figure 3, both tires reach an equal maximum lateral force generation at around 17,350 N. Additionally, the slope of the lateral force vs. slip angle increases, and a more linear-like curve is obtained. Furthermore, the tire shows a normalized lateral force value of 0.86. A similar trend for the cornering stiffness of the standard tire exists between the truckSIM tire model and the measured tire model presented in [36]. It can be seen that the results for the two tire models agree reasonably. As such, the tire model for the axle is substantiated both analytically and using tire data from empirical findings.

3.1 Actuator Force Requirements

A co-simulation of MATLAB-truckSIM was performed to evaluate the effect of the magnitude and rate of applied actuator force tire behavior under the combination of vehicle-load interaction and identify the relevant control scheme. It was determined that the rate of application of actuation force is more influential in conferring stability to the vehicle system than the magnitude of the actuation force alone. The findings were simulated using a single lane change maneuver at 0.4 Hz (equal to 50 degrees of steering wheel angle or 2 degrees of road-wheel steering angle) at 90 km/h. The results of the open-loop test simulated using the nonlinear model were in good agreement with the linear model in section two. As can be seen in Figure 4(a), the trailer yaw rate is effectively diminished.

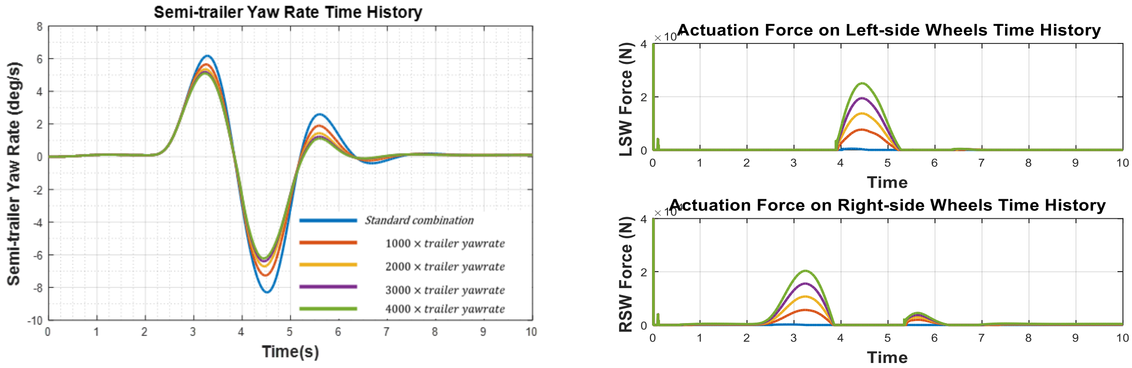

Figure 4. Open-loop performance of active auxiliary axle using truckSIM nonlinear model a) yaw rate performance in single lane change, b) actuator force on the right side (RSW) and left side (LSW) wheels

4.0 DEVELOPMENT OF CONTROL SCHEME

4.1 Yaw Rate Reference

Salaani's steady-state relation [38], developed from a similar 3-DOF AHV model, was adopted as a yaw rate reference to establish the desired yaw rate reference and, subsequently the error criteria from desired conditions. Eq. 4a through 4d represent the steady-state yaw rate, limiting conditions, and the relation for error, respectively.

$$r_{ss} = \frac{v_x \delta}{L + K_u v_x^2}$$

$$K_u = m \frac{\sum_{i=2}^{N}(b_{i-1}C_i) - aC_1}{C_1 \sum_{i=2}^{N}(a + b_{i-1})C_i} + m_1 \left(\frac{\sum_j^M h_j C_{N+j}}{\sum_j^M (h_j + e) C_{N+j}} \right) \frac{\sum_{i=2}^{N}(b_{i-1} - d)C_i - (a + d)C_1}{C_1 \sum_{i=2}^{N}(a + b_{i-1})C_i} \tag{4a}$$

$$L = \frac{\sum_{i=2}^{N} b_{i-1}C_i - aC_1}{C_1 \sum_{i=2}^{N}(a + b_{i-1})C_i} \left(\sum_{i=1}^{N} C_i \left(\frac{\sum_{i=2}^{N} b_{i-1}^2 C_i + a^2 C_1}{\sum_{i=2}^{N} b_{i-1}C_i - aC_1} \right) - \left(\sum_{i=2}^{N} b_{i-1}C_i - aC_1 \right) \right) + \frac{\sum_{i=2}^{N}(b_{i-1} - d)C_i}{C_1 \sum_{i=2}^{N}(a + b_{i-1})C_i} \left(\sum_{j=1}^{M} C_{N+j} \frac{\sum_{j=1}^{M} h_j (h_j + e) C_{N+j}}{\sum_{j=1}^{M} (h_j + e) C_{N+j}} - \sum_{j=1}^{M} h_j C_{N+j} \right)$$

$$|r_{ss}| \leq \frac{\mu g}{v_x} \tag{4b}$$

$$r_{ss} = \begin{cases} r_{ss} & |r_{ss}| < \dfrac{\mu g}{v_x} \\ \dfrac{\mu g}{v_x} & |r_{ss}| \geq \dfrac{\mu g}{v_x} \end{cases} \tag{4c}$$

$$E = r_{actual} - r_{ss} \tag{4d}$$

$$\dot{E} = \dot{r}_{actual} - \dot{r}_{ss} \tag{4e}$$

4.2 Development of Control Scheme

A fuzzy logic control scheme was developed to control the actuation of the active axle in the closed-loop algorithm. In this approach, a multi-input single-output (MISO) system was considered. Figure 5(a) represents the overall control structure for the controller-actuator combination. The inputs to the FLC system are yaw rate and acceleration errors defined by Eq. 4d and Eq. 4e, respectively. The relationship between yaw rate and actuation force was nonlinear, such that higher yaw rates required faster and not necessarily higher magnitudes of actuation. More clearly, for a given magnitude of actuator force bounded by the maximum vertical force the tire can withstand, the rate at which the actuation force is developed and transmitted to the tire is much more influential in conferring stability than the magnitude of the force itself. Thus, the acronym RDFLC stands for rate-dependent fuzzy logic controller. The output of the system represents the rate at which the actuation force has to be administered. The Takagi-Sugeno approach was used to design the fuzzy logic controller with the output ranging between -1 and 1. In this respect, -1 implies the highest rate of reduction of actuation force, while +1 represents the highest rate of application of actuation force. An empirical gain is introduced to amplify the output to meet the boundaries of actuation force magnitude. The membership functions are introduced in Figures 5(b) and Figure 5(c), respectively.

In the existing notations, NB, NM, NS, Z, PS, PM, and PB represent negative big, negative medium, negative small, zero, positive small, positive medium, and positive big. The rows in Table 2 demonstrate the contributions of yaw rate error, while the columns illustrate yaw acceleration error, respectively.

The axle configuration is semi-active, with conventional springs and hydraulic actuators replacing the original hydraulic shock absorbers. To this end, the function of the axle-controller configuration is very similar to an axle equipped with active anti-roll bars (ARB). However, since the axle is not originally in contact with the road, the actuation through hydraulic cylinders causes vibrations at the road-tire contact. The PID controller here is a lower-level controller that regulates the actuation force administered by the higher-level FLC controller system. As such, we adopted an FLC controller to regulate the rate of actuation force, and we adopted a lower-level PID to regulate the real-time magnitude of the force. The PID coefficients were derived empirically. The values of the coefficients have been set to P=100, I=15, and D=0.01, respectively. In the derivation of the values, the authors aimed to achieve minimum time for a stable force distribution at the tire contact patch.

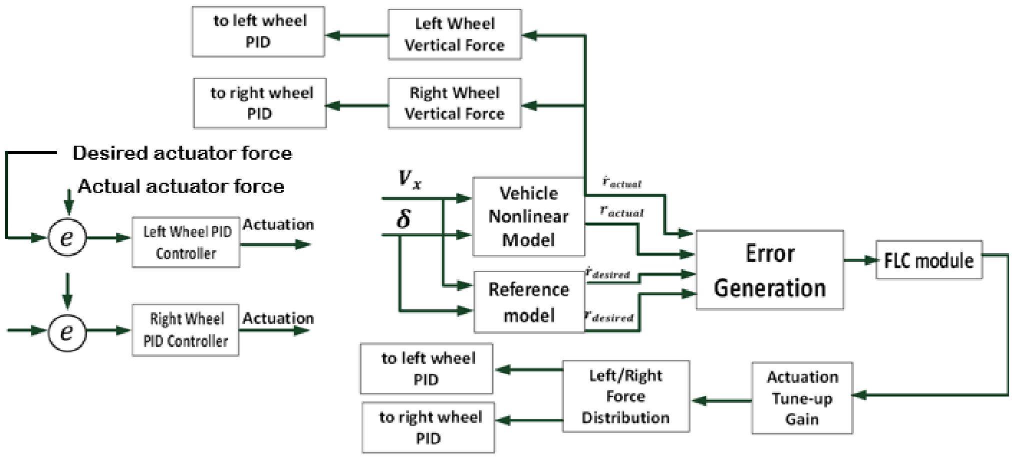

(a)

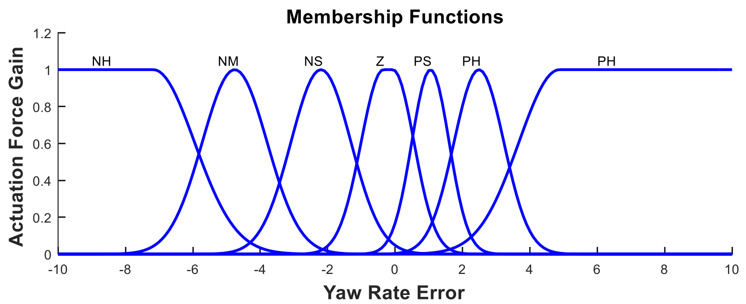

(b)

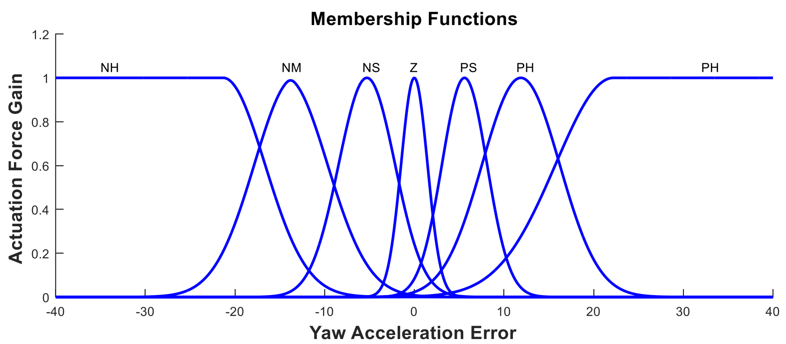

(c)

Figure 5. (a) Control system structure for active auxiliary axle (b) Membership functions of the yaw rate error (c) Membership functions of the error yaw acceleration error

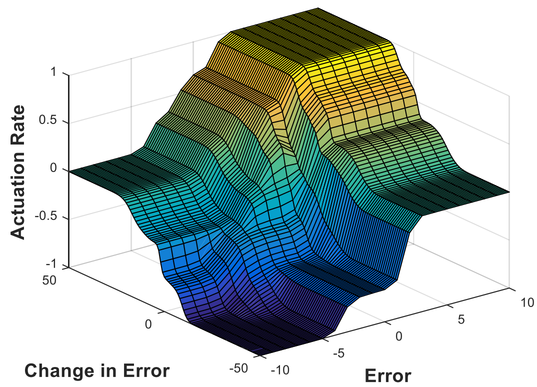

(d)

Figure 5. (cont.) (d) 3D surface representing the input-output relationship

Table 2. Rule base for the fuzzy logic system

e \ e	NB	NM	NS	Z	PS	PM	PB
NB	NB	NB	NM	NM	NM	NB	ZE
NM	NB	NM	NM	NM	NS	PS	PS
NS	NM	NS	NS	NS	ZE	PS	PS
Z	NM	NS	ZE	ZE	ZE	PM	PM
PS	NS	NS	ZE	PS	PS	PM	PM
PM	NS	NS	ZE	PM	PM	PB	PB
PB	ZE	ZE	PS	PM	PM	PB	PB

5.0 DEVELOPMENT OF CONTROL SCHEME

The effectiveness of the controller-actuator system was evaluated in a co-simulation of TruckSIM and Matlab/SIMULINK using a driver-implemented PID model to simulate a double lane change maneuver at 90 km/h with a peak amplitude of 4.5 degrees of the steering wheel at the trailer front axle. Two loading conditions that provoke instability were considered, such as the vehicle experiencing LOC (lateral swing and single-wheel lift-off). Vehicle forward speed and coefficient of road friction were considered 90 km/h and 0.85, respectively. Loading and friction conditions for each maneuver are summarized in Table 3.

Table 3. Loading conditions of the tractor semi-trailer in the DLC maneuver

Parameters	Maneuver Scenario	
	I	II
Mass of cargo load	7000kg	7000kg
Distance behind hitch point	4500 mm	8000
Coefficient of road friction	0.85	0.85

5.1 Maneuver Scenario I

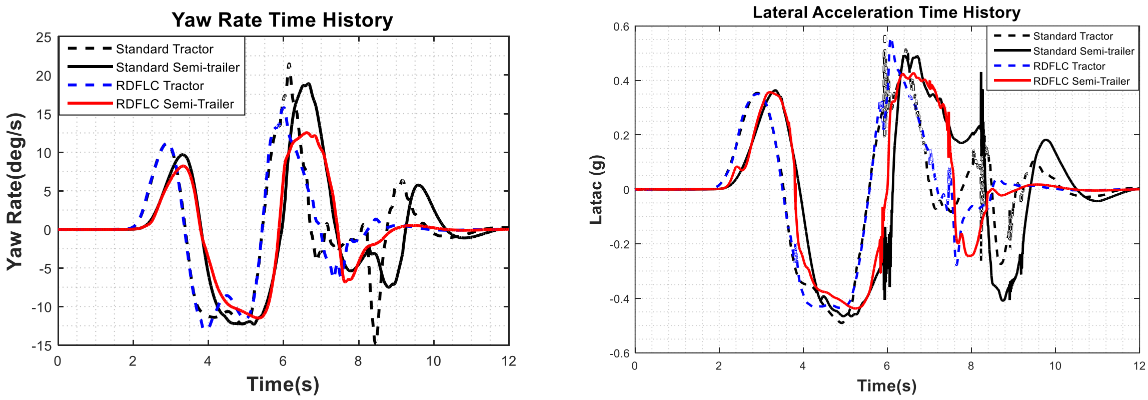

(a) (b)

Figure 6. The effect of active axle intervention using a fuzzy logic controller in a double lane change maneuver with 7000kg of payload at 4500mm behind hitch point location, (a) yaw rate, (b) lateral acceleration

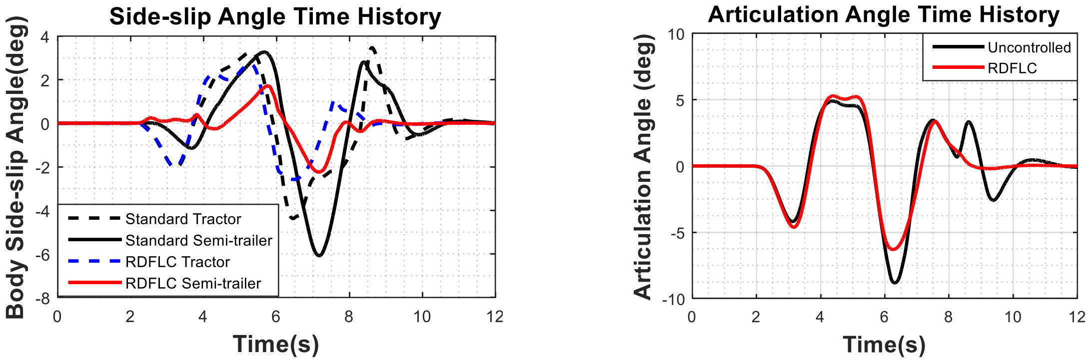

Figure 6. (cont.) (c) vehicle body side slip angle and (d) articulation angle

5.2 *Maneuvre Scenario* II

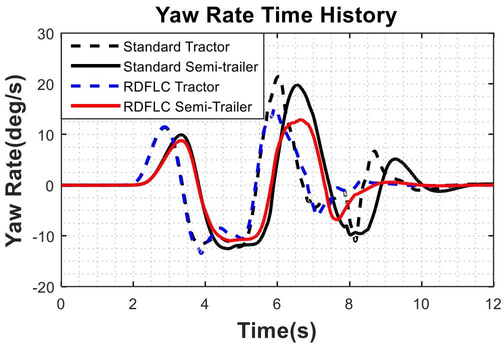

(a)

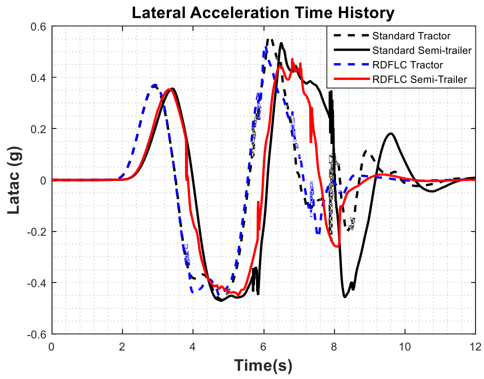

(b)

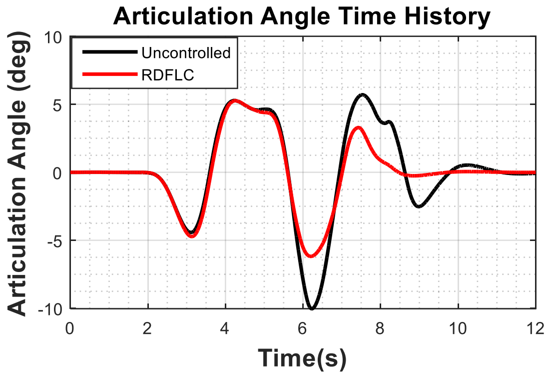

(c)

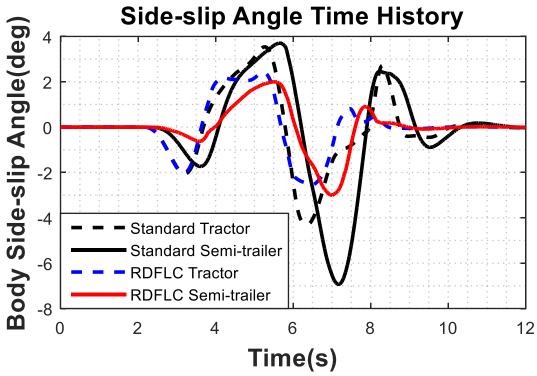

(d)

Figure 7. The effect of active axle intervention using a fuzzy logic controller in a double lane change maneuver with 7000kg of payload at 8000mm behind hitch point location (a) yaw rate, (b) lateral acceleration, (c) vehicle body side slip angle and (d) articulation angle

Figures 6 and 7 represent the simulated results of the two loading conditions for yaw rate, lateral acceleration, articulation angle, and vehicle body side-slip angles, respectively. It can be seen from the lateral acceleration time history that the loading conditions have successfully fulfilled the requirements to confer instability to the uncontrolled combination without causing absolute rollover or jack-knifing, thus effectively simulating the conditions preliminarily hypothesized for loss of control in the lateral direction. The loading conditions additionally simulate a lightly loaded trailer, which is most prone to exhibit lateral instability.

The proposed system has effectively stabilized the combination even past the completion of the lane change, where overshoots in yaw rate and lateral acceleration continue to exist. Referring to the articulation angle time history, the intervention of the controller-actuator combination has successfully improved handling performance and has helped the vehicle negotiate the maneuver by reducing trailer oscillations. This is important because handling performance and stability are two characteristics that demonstrate opposite behavior when the intervention of an auxiliary system is introduced in favor of one. Nonetheless, since the current scenario considers instability beyond the handling limit, an improvement in stability has resulted in the vehicle regaining handling. Lateral acceleration and yaw rate time histories clearly illustrate the prevalent rearward amplification (the ratio of maximum yaw rate and lateral acceleration of the semi-trailer to the tractor) and how it is effectively diminished by the active auxiliary axle.

Most notably, the intervention of the active auxiliary axle has not only helped the trailer recover from the combined lateral and relative roll instability (single-wheel lift-off at the tractor front axle) but also helped the towing unit stabilize and regain control over the course of the maneuver. Referring to yaw rate and articulation angle responses in both maneuvers, it can be seen that the active axle serves to stabilize the tractor accordingly. This is considerably important because at handling limits of such severity, where the loss of contact is an inevitable contributor to complex multi-directional destabilization, the successful functioning of other yaw stability systems, including differential braking and active steering, may degrade severely due to dependence on the original tire-road contact.

In contrast with minimal improvement in the mid-maneuver yaw rate response, post-maneuver oscillations have diminished substantially. This can be attributed to two factors: first, while steering angle alterations for both cases within the mid-maneuver period represent minimal discrepancy, the yaw rate experienced in the standard combination can be claimed to be the natural yaw rate required to negotiate the maneuver without the driver's attempt to slow the vehicle down. The similarity in the shape of the yaw rate response for both loading combinations dictates that within the region under consideration, loading cannot affect the yaw rate response. Past this range and over the second half-maneuver section, the intervention of the active axle considerably reduces the lateral acceleration by 0.2 g for both cases. This coincides with the region where single-wheel lift-off is successfully prevented, and the driver attains natural control over the steering wheel. Table 3 offers a comparison of the improvement in vehicle states in percentage values and their interaction with one another.

6.0 CONCLUSION

The aim of the current paper was to mitigate the lateral instability of a tractor semi-trailer combination at the instant of loss of control in the lateral direction by introducing a new trailer-based approach. The hypothesis underlying the approach followed herein was based on available research on factors affecting AHV stability, including tire cornering force generation behavior, suspension roll stiffness distribution, and yaw rate dependency of lateral stability. In this regard, a linear model was developed to examine the potential of introducing a low-complexity retrofit to the towed unit to maintain stability after a loss of control is experienced. Severe double lane change maneuvers at 90 km/h with a closed-loop driver model to maintain the steering wheel in combination with two loading conditions successfully simulated instability cases with the trailer exhibiting lateral swing and the tractor experiencing single-wheel lift-off (relative roll-over). The intervention of the active axle effectively damped yaw rate and lateral acceleration peaks without adversely affecting the mid-maneuver response, suggesting lateral stabilizing efficiency without compromising handling performance. Additionally, the results suggest that there is a collateral benefit of rollover prevention due to reduced lateral acceleration and controlled single-wheel lift-off returning to road-holding in the tractor's front axle. The findings of the current paper put forward a promising approach to the minimal retrofit required to achieve considerable improvement in traffic safety imposed by the lateral instability of AHVs.

7.0 REFERENCES

[1] H. A. Jeyed, and A. Ghaffari, "Nonlinear estimator design based on extended Kalman filter approach for state estimation of articulated heavy vehicle." *Proceedings of the Institution of Mechanical Engineers, Part K: Journal of Multi-body Dynamics*, vol. 233, no. 2, pp. 254-265, 2019.

[2] B. Ji-hua, L. Jin-liang, and Y. Yan. "Lateral stability analysis of the tractor/full trailer combination vehicle," *2011 International Conference on Electric Information and Control Engineering*, pp. 2294-2298, 2011.

[3] P. S. Fancher, "The static stability of articulated commercial vehicles," *Vehicle System Dynamics*, vol. 14, no. 4-6, pp. 201-227, 1985.

[4] A. Stribersky, and P. S. Fancher, "The nonlinear behavior of heavy-duty truck combinations with respect to straightline stability," vol. 111, no. 4, pp. 577-582, 1989.

[5] R. Scheidl, A. Stribersky, H. Troger, K. Zeman, "Driving behavior of a tractor-semitrailer vehicle in steady state downhill motion," *Vehicle System Dynamics*, vol. 14, no. 1-3, pp. 184-188, 1985.

[6] R. D. Ervin, R. L. Nisonger, C. Mallikarjunarao and T. D. Gillespie, The yaw stability of tractor-semitrailers during cornering, Final report, University of Michigan, 1979.

[7] C. Winkler, P. Fancher, C. MacAdam, "Parametric analysis of heavy duty truck dynamic stability," vol. 1, Technical Report, National Highway Traffic Safety Administration, 1983.

[8] C. Cheng, R. Roebuck, A. Odhams and D. Cebon, "High-speed optimal steering of a tractor–semitrailer," *Vehicle System Dynamics*, vol. 49, no. 4, pp. 561-593, 2011.

[9] S. H. Tabatabaei, A. Zahedi and A. Khodayari, "The effects of the Cornering Stiffness variation on Articulated Heavy Vehicle stability," 2012 IEEE International Conference on Vehicular Electronics and Safety, Istanbul, Turkey, pp. 78-83, 2012.

[10] D. Elsasser, F. S. Barickman, H. Albrecht, J. Church, G. Xu and M. Heitz "Tractor semitrailer stability objective performance test research–Yaw stability," Technical Report, National Highway Traffic Safety Administration, 2013.

[11] M. Ei-Gindy, N. Mrad, and X. Tong, "Sensitivity of rearward amplication control of a truck/full trailer to tyre cornering stiffness variations," *Proceedings of the Institution of Mechanical Engineers, Part D: Journal of Automobile Engineering*, vol. 215, no. 5, pp. 579-588, 2001.

[12] H. B. Pacejka, Tire and vehicle dynamics, Elsevier, 2012.

[13] D. H. Wu, and J. Hai, "Analysis of dynamic lateral response for a multi-axle-steering tractor and trailer," *International Journal of Heavy Vehicle Systems*, vol. 10, no. 4, pp. 281-294, 2003.

[14] B. Jujnovich, R. Roebuck, A. Odhams, and D. Cebon, "Implementation of active rear steering of a tractor semi-trailer," *International Conference on Heavy Vehicles Transport Technology*, Paris. 2008.

[15] K. Rangavajhula, and H. S. Jacob Tsao, "Effect of multi-axle steering on off-tracking and dynamic lateral response of articulated tractor-trailer combinations," *International Journal of Heavy Vehicle Systems*, vol. 14, no. 4, pp. 376-401, 2007.

[16] L. Palkovics, and A. Fries, "Intelligent electronic systems in commercial vehicles for enhanced traffic safety," *Vehicle System Dynamics*, vol. 35, no. 4-5, pp. 227-289, 2001.

[17] C. Cheng, R. Roebuck, A. Odhams, D. Cebon, "High-speed optimal steering of a tractor–semitrailer," *Vehicle system dynamics*, vol. 49, no. 4, pp. 561-593, 2011.

[18] C. Cheng and D. Cebon, "Improving roll stability of articulated heavy vehicles using active semi-trailer steering," *Vehicle System Dynamics*, vol. 46, no. S1, pp. 373-388, 2008.

[19] S. H. T. Oreh, R. Kazemi, and S. Azadi, "A new desired articulation angle for directional control of articulated vehicles," *Proceedings of the Institution of Mechanical Engineers, Part K: Journal of Multi-body Dynamics*, vol. 226, no. 4, pp. 298-314, 2012.

[20] S. H. T. Oreh, R. Kazemi, S. Azadi and A. Zahedi, "A new method for directional control of a tractor semi-trailer," *Australian Journal of Basic and Applied Sciences*, vol. 6, no. 12, pp. 396-409, 2012.

[21] S. Zhu, H. Yuping, and R. Jing, "On robust controllers for active steering systems of articulated heavy vehicles," *International Journal of Heavy Vehicle Systems*, vol. 26, no. 1, pp. 1-30, 2019.

[22] Goodarzi, Avesta, Javad Mehrmashhadi, and Ebrahim Esmailzadeh. "Optimised braking force distribution strategies for straight and curved braking." *International Journal of Heavy Vehicle Systems*, vol. 16, no.1-2, pp. 78-101, 2009.

[23] A. Goodarzi, M. Behmadi, and E. Esmailzadeh, "An optimised braking force distribution strategy for articulated vehicles," *Vehicle System Dynamics*, vol. 46, no. S1, pp. 849-856, 2008.

[24] F. Mobini, A. Ghaffari, and M. Alirezaei, "Non-linear optimal control of articulated-vehicle planar motion based on braking utilizing the state-dependent Riccati equation method," *Proceedings of the Institution of Mechanical Engineers, Part D: Journal of Automobile Engineering*, vol. 229, no. 13, pp. 1774-1787, 2015.

[25] X. Yang, "Optimal reconfiguration control of the yaw stability of the tractor-semitrailer vehicle," *Mathematical Problems in Engineering*, vol. 2012, p. 602502, 2012.

[26] C. Zong, T. Zhu, C. Wang and H. L. Zong, "Multi-objective stability control algorithm of heavy tractor semi-trailer based on differential braking," *Chinese Journal of Mechanical Engineering*, vol. 25, no. 1, pp. 88-97, 2012.

[27] A. Goodarzi, M. Behmadi and E. Esmailzadeh, "Optimized braking force distribution during a braking-in-turn maneuver for articulated vehicles," *2010 International Conference on Mechanical and Electrical Technology*, Singapore, pp. 555-559, 2010.

[28] X. Yang, S. Juntao and J. Gao, "Fuzzy logic based control of the lateral stability of tractor semitrailer vehicle," *Mathematical Problems in Engineering*, vol. 2015, p. 692912, 2015.

[29] D. J. M. Sampson, and D. Cebon, "Achievable roll stability of heavy road vehicles," *Proceedings of the Institution of Mechanical Engineers, Part D: Journal of Automobile Engineering*, vol. 217, no. 4, pp. 269-287, 2003.

[30] H. H. Huang, R. K. Yedavalli, and D. A. Guenther, "Active roll control for rollover prevention of heavy articulated vehicles with multiple-rollover-index minimisation," *Vehicle System Dynamics*, vol. 50, no. 3, pp. 471-493, 2012.

[31] H. A. Jeyed and A. Ghaffari, "Nonlinear estimator design based on extended Kalman filter approach for state estimation of articulated heavy vehicle," *Proceedings of the Institution of Mechanical Engineers, Part K: Journal of Multi-body Dynamics*, vol. 233, no. 2, pp. 254-265, 2019.

[32] F. M. Barbosa, L. B. Marcos, M. M. da Silva, M. H. Terra, and V. G. Junior, "Robust path-following control for articulated heavy-duty vehicles," *Control Engineering Practice*, vol. 85, pp. 246-256, 2019.

[33] X. Xu, L. Zhang, Y. Jiang and N. Chen, "Active control on path following and lateral stability for truck–trailer combinations," *Arabian Journal for Science and Engineering*, vol. 44, pp. 1365-1377, 2019.

[34] M. Zanchetta, D. Tavernini, A. Sorniotti, et al., "Trailer control through vehicle yaw moment control: Theoretical analysis and experimental assessment," *Mechatronics*, vol. 64, p.102282, 2019.

[35] Y. Zhang, A. Khajepour, E. Hashemi, Y. Qin and Y. Huang, "Reconfigurable model predictive control for articulated vehicle stability with experimental validation," *IEEE Transactions on Transportation Electrification*, vol. 6, no. 1, pp. 308-317, 2019.

[36] J. Y. Wong, Theory of ground vehicles, John Wiley & Sons, 2008.

[37] B. Mashadi, M. I. Assadia and S. K. Bidhendib, "Active Auxiliary Tag Axle: A new approach to lateral stabilization of articulated heavy vehicles," *6th International Conference on Acoustics and Vibration*, Tehran, Iran, no. 6286, 2016.

[38] M. K. Salaani, "The application of understeer gradient in stability analysis of articulated vehicles," *International Journal of Heavy Vehicle Systems*, vol. 16, no. 1-2, pp. 3-25, 2009.